Continental-scale decrease in net primary productivity in streams due to climate warming

Song, Chao; Dodds, Walter K.; Rüegg, Janine; Argerich, Alba; Baker, Christina L.; Bowden, William B.; Douglas, Michael M.; Farrell, Kaitlin J.; Flinn, Michael B.; Garcia, Erica A.; Helton, Ashley M.; Harms, Tamara K.; Jia, Shufang; Jones, Jeremy B.; Koenig, Lauren E.; Kominoski, John S.; McDowell, William H.; McMaster, Damien; Parker, Samuel P.; Rosemond, Amy D.; Ruffing, Claire M.; Sheehan, Ken R.; Trentman, Matt T.; Whiles, Matt R.; Wollheim, Wilfred M.; Ballantyne, Ford

Published in:
Nature Geoscience

DOI:
10.1038/s41561-018-0125-5

Published: 21/05/2018

Document Version
Peer reviewed version

Continental-scale decrease in net ecosystem productivity in streams due to climate warming

Chao Song[1], Walter K. Dodds[2], Janine Rüegg[2,3], Alba Argerich[4,5], Christina L. Baker[6], William B. Bowden[7], Michael M. Douglas[8], Kaitlin J. Farrell[1,9], Michael B. Flinn[10], Erica A. Garcia[11], Ashley M. Helton[12], Tamara K. Harms[6], Shufang Jia[2], Jeremy B. Jones[6], Lauren E. Koenig[12,13], John S. Kominoski[1,14], William H. McDowell[13], Damien McMaster[11], Samuel P. Parker[7], Amy D. Rosemond[1], Claire M. Ruffing[2,6], Ken R. Sheehan[13,15], Matt T. Trentman[2,16], Matt R. Whiles[17], Wilfred M. Wollheim[13], and Ford Ballantyne IV[1].

[1]Odum School of Ecology, University of Georgia, Athens, GA 30602, USA. [2]Division of Biology, Kansas State University, Manhattan, KS 66506, USA. [3]Stream Biofilm and Ecosystem Research Laboratory, École Polytechnique Fédérale de Lausanne, CH–1015 Lausanne, Switzerland. [4]Department of Forest Engineering, Resources, and Management, Oregon State University, Corvallis, OR 97731, USA. [5]School of Natural Resources, University of Missouri, Columbia, MO 65211, USA. [6]Department of Biology and Wildlife and Institute of Arctic Biology, University of Alaska Fairbanks, Fairbanks, AK 99775, USA. [7]Rubenstein School of Environment and Natural Resources, University of Vermont, Burlington, VT 05401, USA. [8]School of Biological Sciences, and School of Agriculture and Environment, University of Western Australia, Perth, WA 6009, Australia. [9]Department of Biological Sciences, Virginia Polytechnic Institute and State University, Blacksburg, VA 24061, USA. [10]Biological Sciences, Murray State University, Murray, KY 42071, USA. [11]Research Institute for the Environment and Livelihoods, Charles Darwin University, Darwin, Northern Territory 0909, Australia. [12]Department of Natural Resources and the Environment, and the Center for Environmental Sciences and Engineering, University of Connecticut, Storrs, CT 06269, USA. [13]Department of Natural Resources and the Environment, University of New Hampshire, Durham, NH 03824, USA. [14]Department of Biological Sciences, Florida International University, Miami, FL 33199, USA. [15]Southwest Biological Science Center, United States Geological Survey, Flagstaff, AZ 86001, USA. [16]Department of Biological Sciences, University of Notre Dame, Notre Dame, IN 46556, USA. [17]Department of Zoology and Center for Ecology, Southern Illinois University, Carbondale, IL 62901, USA.

Main text

Streams play a key role in the global carbon cycle. The balance between carbon intake through photosynthesis and carbon release via respiration influences carbon emissions from streams and depends on temperature. However, the lack of a comprehensive analysis of the temperature sensitivity of the metabolic balance in inland waters across latitudes and local climate conditions hinders an accurate projection of carbon emissions in a warmer future. Here, we use a model of diel dissolved oxygen dynamics, combined with high-frequency measurements of dissolved oxygen, light, and temperature, to estimate the temperature sensitivities of gross primary production and ecosystem respiration in streams across six biomes, from the tropics to the arctic tundra. We find that the change in metabolic balance, that is, the ratio of gross primary production to ecosystem respiration, is a function of stream temperature and current metabolic balance. Applying this relationship to the global compilation of stream metabolism data, we find that a 1 °C increase in stream temperature leads to a convergence of metabolic balance, and to a 23.6% overall decline in net ecosystem productivity across the streams studied. We suggest that if the relationship holds for similarly-sized streams around the globe, the warming-induced shifts in metabolic balance will result in an increase of 0.0194 Pg carbon emitted from such streams every year.

Streams play a significant role in the transport, storage, and transformation of organic carbon globally[1,2]. Recent estimates suggest that 0.8–1.8 petagrams (Pg) of carbon evade from streams and rivers to the atmosphere annually[3,4]. This is comparable in size to the net annual terrestrial–atmosphere and net ocean–atmosphere carbon exchange[5]. Stream metabolism, which is governed by gross primary production (GPP) and ecosystem respiration (ER), contributes substantially to the overall carbon flux out of streams. A recent study estimated that stream metabolism is responsible for up to 28% of the total carbon flux from streams to the atmosphere[6], resulting in an estimated net flux of 0.12 Pg C per year[7]. As GPP and ER are both temperature dependent processes, sustained climate warming has the potential to profoundly alter the rates of carbon flux in and out of streams. Over the past century, mean water temperature in US rivers and streams increased at a rate of 0.009–0.077 °C per year[8], and stream temperatures are predicted to increase by 1–3 °C with the doubling of atmospheric CO_2 concentration[9]. Consequently, understanding the feedback between stream metabolism and global warming is crucial when considering global or regional carbon cycles.

Although it is tempting to use well quantified temperature responses of photosynthesis and respiration at the cellular level to predict ecosystem–level responses to warming, complex interactions among organisms and their abiotic environments can confound the temperature responses of cellular processes at higher levels of organization. Taken at face value, the differential temperature sensitivities of photosynthesis and respiration at the cellular level defined by activation energy in the Arrhenius equations ($\approx$ 30.9 and 62.7 KJ mol^{-1} for photosynthesis and respiration, respectively[10]) prescribe a relatively faster increase in ER than GPP in response to warming. Consequently, we would predict that streams will become more heterotrophic (i.e. lower GPP/ER) as climate continues to warm. However, the implicit assumption of such a prediction, that the activation energies of photosynthesis and respiration at the cellular level are appropriate for describing the temperature sensitivities of GPP and ER in streams at the ecosystem level, may not hold.

Intrinsic variation in the temperature dependence of multiple processes that comprise aggregated ecosystem rates can cause the temperature sensitivities of whole ecosystem processes to deviate from the temperature dependence of cellular level responses. For example, variation in algal community composition can influence the temperature sensitivity of ecosystem–level GPP because the activation energy of photosynthesis varies across phyla of algae[11,12]. Similarly, the chemical structure of organic compounds influences the activation energy of decomposition reactions, and thus, variation in respiratory substrate composition can affect the temperature sensitivity of ER[13]. Alternatively, if ecosystem–level GPP and ER are influenced by other temperature dependent processes, inferred temperature sensitivities of GPP and ER may reflect the influences of these processes and not necessarily the temperature sensitivities of cellular photosynthesis and respiration. For example, warming may accelerate the flux of nutrients and organic carbon from sediments to the water column[14] and transport of nutrients across cell membranes[15], both of which could result in amplified temperature sensitivities at the ecosystem level[16]. Temperature sensitivities of GPP and ER may reflect the temperature sensitivity of a process that constrains GPP or ER, such as nitrogen supply[19]. Conversely, the temperature sensitivities of GPP or ER at the ecosystem level can be muted by nutrient limitation[17,18]. Finally, variation in the responses of different taxa to temperature variation can confound aggregate temperature sensitivity. Differential responses to warming across decomposer taxa have even been shown to cancel each other out, resulting in no net change in ecosystem carbon flux in response to warming[20].

In addition to the inherent complexity in ecosystem–level temperature sensitivities of GPP and ER, the varied approaches employed to quantify them also have the potential to influence the inferred ecosystem–level temperature dependence of GPP and ER. Incubations of stream substrata at different temperatures[21,22] or mesocosm warming experiments[23] do not include the entire focal ecosystem and may not encompass the processes key for determining the temperature sensitivities of GPP and ER at the ecosystem level. Comparisons among streams or within one stream over seasons[19,24–28] yield ecosystem–level estimates of temperature sensitivities, but temperature independent differences among streams or seasons due to hydrology[29], geomorphology[22], nutrient availability[30,31], and light availability[26] can easily confound the responses of GPP and ER to temperature. These confounding factors render the estimated temperature dependence not purely a response to temperature, but an integrated response to the suite of temperature dependent and independent differences across streams or seasons.

Given the complexity of ecosystem–level temperature sensitivities and the challenges associated with quantifying them, it is not surprising that various patterns have been reported. Some studies have found consistent temperature sensitivities of ER at the ecosystem and the cellular levels[21,23,27,28], but others have demonstrated considerable deviation of ecosystem–level activation energies of GPP[23,27,32] and ER[19,25] from the values of their cellular analogs. In studies that simultaneously examined the temperature dependence of GPP and ER in streams, a shift toward heterotrophy with warming has been observed in some instances[23,27], but a recent synthesis based on geothermal streams concluded that warming increases GPP and ER to the same extent and results in no net change in metabolic balance[32]. To date, simultaneous quantification of the temperature dependence of GPP and ER have been constrained to mesocosm incubations or geothermal streams. Thus, there is still uncertainty about whether streams will become more heterotrophic (decreasing GPP/ER and NEP) or more autotrophic (increasing GPP/ER and NEP) at the continental scale in response to continued warming. Simultaneously quantifying the ecosystem–level temperature sensitivities of GPP and ER in streams across broad bio-climatic regions is key to resolving such uncertainty.

Here, we estimate the temperature sensitivities of GPP and ER in streams from six distinct biomes. We utilize the response of DO concentration to diel temperature variation and dynamic models of DO concentration to infer the temperature dependence of GPP and

ER for each stream over multiple days[33]. Compared to studies that analyze streams along spatial or seasonal temperature gradients, we avoid the implicit assumption that differences in stream metabolism along the temperature gradient are mainly attributed to temperature differences, and thus minimize the influence of factors that covary spatially or seasonally with temperature[34]. Moreover, this dynamic modeling approach allows us to estimate temperature dependence of GPP and ER for each stream, and thus characterize stream to stream variation in the temperature sensitivity of whole stream metabolism. Combining dynamic models with high resolution time series of light, temperature, and DO in streams across six biomes allows us to quantify the temperature dependence of stream metabolism across latitude, and refine predictions of the feedback between stream metabolic balance and global warming.

Estimating activation energies of GPP and ER

We estimated the ecosystem–level activation energies of GPP and ER in streams across six biomes by modeling diel changes in DO concentration. The six distinct biomes that span a wide range of latitude (13°S – 68 °N) include tropical forest (Luquillo Experimental Forest, Puerto Rico (LUQ)), tropical savanna (Litchfield National Park, North Territory, Australia (AUS)), tallgrass prairie (Konza Prairie, Kansas, USA (KNZ)), temperate rainforest (Andrews Experimental Forest, Oregon, USA (AND)), boreal forest (Caribou-Poker Creeks Research Watershed, Alaska, USA (CPC)), and arctic tundra (Toolik Lake Field Station, Alaska, USA (ARC)). In each biome, we measured DO concentration, photosynthetically active radiation, and water temperature at a 5 or 10 minute interval for 1–2 weeks in multiple stream reaches throughout a watershed. We modeled the response of DO concentration to diel temperature variation to estimate ecosystem–level activation energies of GPP and ER. Specifically, we modeled the dynamics of DO concentration as:

$$\frac{d[\mathrm{O}_2]}{dt} = GPP - ER + K([\mathrm{O}_2]_{sat} - [\mathrm{O}_2]). \quad (1)$$

Here, $[\mathrm{O}_2]_{sat}$ is the saturated DO concentration and can be calculated from temperature and barometric pressure[35]. GPP, ER, and K are instantaneous rates of primary production, respiration, and reaeration respectively. We modified previously published models of aquatic metabolism[36–38] by using the Arrhenius equation to describe the temperature dependence of GPP and ER. Specifically, GPP, ER, and K were modeled as :

$$GPP = P_{max}\tanh(\frac{\alpha I}{P_{max}})e^{-\frac{Eap}{R}(\frac{1}{T}-\frac{1}{T_0})}; \quad (2)$$

$$ER = R_{T_0} e^{-\frac{Ear}{R}(\frac{1}{T}-\frac{1}{T_0})}; \quad (3)$$

$$K = K_{20} \times 1.024^{T-20}. \quad (4)$$

Here, P_{max} (mg O_2 L^{-1} min^{-1}) is the maximum primary production rate, α (mg O_2 L^{-1} s m^{-2} μE^{-1} min^{-1}) is the slope of the light response curve of primary production at low light intensity, R_{T_0} (mg O_2 L^{-1} min^{-1}) is the respiration rate at reference temperature T_0 (Kelvin), which we set at the average daily water temperature across all days for each stream reach, K_{20} (min^{-1}) is the reaeration coefficient at 20 °C, I (μE m^{-2} s^{-1}) is photosynthetically active radiation, T (Kelvin) is water temperature, R (8.314 KJ mol^{-1} $Kelvin^{-1}$) is the ideal gas constant, E_{ap} (KJ mol^{-1}) and E_{ar} (KJ mol^{-1}) are the activation energies of GPP and ER, respectively. We employed a Bayesian approach to estimate the parameters (P_{max}, α, R_{T_0}, K_{20}, E_{ap}, E_{ar}) in the model[39], and calculated daily GPP, ER, GPP/ER, and NEP using the estimated parameters and associated light and temperature profiles (see methods).

The estimated ecosystem–level activation energies exhibited significant variability both within and across biomes (Fig. 1), and were not significantly correlated with GPP, ER, or NEP (Fig. S1–S3). The activation energies of GPP and ER varied substantially from the activation energies of photosynthesis and respiration at the cellular level. Specifically, activation energies ranged from 0.5 to 839.2 KJ mol^{-1} for GPP and from 0.4 to 837.2 KJ mol^{-1} for ER. The median activation energies of GPP and ER were 68.2 KJ mol^{-1} and 67.5 KJ mol^{-1}, respectively, which is consistent with a recent study quantifying the temperature sensitivity of GPP and ER in streams along a geothermal gradient[32]. However, this does not necessarily imply that warming will increase GPP and ER to the same extent. Due to the nonlinear nature of temperature dependence and substantial variability in the activation energies of GPP and ER, simply using the central tendency of the estimated activation energies will not accurately describe the thermal response of stream metabolism within and across biomes. The inherent variation in activation energies underscores the importance of quantifying the thermal response of stream metabolism using activation energies of GPP and ER for individual streams rather than using the mean or median activation energies across all streams.

Activation energy of GPP/ER decreases with GPP/ER and temperature

The simultaneous quantification of the activation energies of GPP and ER allowed us to evaluate thermal response of stream metabolic balance across biomes. A common measure

of metabolic balance in streams is the ratio of GPP to ER, which, for our formulation of the instantaneous rates of GPP and ER, is:

$$\frac{GPP}{ER} = \frac{P_{max}\tanh(\frac{\alpha I}{P_{max}})}{R_{T_0}} e^{-\frac{E_{ap}-E_{ar}}{R}(\frac{1}{T}-\frac{1}{T_0})}. \quad (5)$$

The formulation of GPP/ER has the form of an Arrhenius equation, and thus, $E_{ap} - E_{ar}$ is the apparent activation energy of GPP/ER and determines how instantaneous metabolic balance changes with temperature. A positive $E_{ap} - E_{ar}$ means that GPP/ER will increase as temperature increases and a negative $E_{ap} - E_{ar}$ means GPP/ER will decrease as temperature increases.

Despite significant variation in both E_{ap} and E_{ar} (Fig. 1) and a lack of correlation between E_{ap}, E_{ar}, and GPP, ER, and NEP (Fig. S1–S3), we observed that $E_{ap} - E_{ar}$ decreases significantly with daily GPP/ER (Fig. 2(a); linear mixed effects model, $F_{1,39.14} = 8.23$, $P = 0.0066$) and daily mean water temperature (Fig. 2(b); linear mixed effects model, $F_{1,44.28} = 8.4$, $P = 0.0058$). The negative correlation between $E_{ap} - E_{ar}$, GPP/ER and stream temperature gives rise to a prediction for how metabolic balance will change in response to warming. Specifically, GPP/ER in streams with higher temperature and higher current GPP/ER is predicted to decrease in response to warming, whereas in streams with lower temperature and lower current GPP/ER it is expected to increase. The exact pattern of changes in stream metabolic balance globally will depend on the effect sizes of GPP/ER and temperature, as well as the spatial distribution of temperature and daily GPP/ER around the globe.

We hypothesize that the negative relationship between $E_{ap} - E_{ar}$ and GPP/ER may stem from competition and coexistence among autotrophs and heterotrophs in the benthic community. Because a higher activation energy means a greater relative increase in reaction rates in response to warming[40], it allows organisms with high temperature sensitivity to grow more quickly as temperature increases. Thus, it is possible for organisms with lower metabolic rated and higher thermal responsiveness to compete and coexist with those having higher metabolic rated but lower thermal responsiveness in a fluctuating environment[41,42]. More generally, the tradeoff between rate and responsiveness to temperature can be viewed as an example of nonlinearity of competition as a coexisting mechanism[43].

Warming induces asymmetric convergence in stream metabolic balance

Since activation energy is proportional to the percentage change in reaction rate in an Arrhenius equation[40], the fact that daily GPP/ER and temperature predict $E_{ap} - E_{ar}$ indicates that they also predict the percentage change in GPP/ER (ΔGPP/ER) as temperature increases. We performed a simulated warming experiment to calculate ΔGPP/ER under 1 °C warming, and established a relationship between ΔGPP/ER and predictors of $E_{ap} - E_{ar}$, namely daily GPP/ER and mean water temperature. Specifically, we added 1 °C to each recorded water temperature, which represents a realistic estimate of stream temperature in the next century[8]. Using the observed light trajectories, the elevated temperature trajectories, and parameters in the DO model (equation 1–4) estimated from field data, we calculated the daily GPP, ER and then the proportional change in GPP/ER (ΔGPP/ER) under this warming scenario for each stream in our data set. We analyzed the effects of daily GPP/ER and mean water temperature on ΔGPP/ER in a linear mixed effects model. As expected, ΔGPP/ER decreased significantly with both daily GPP/ER (Fig 3(a), $F_{1,39.29} = 12.50$, $P = 0.0011$) and temperature (Fig 3(b), $F_{1,42.41} = 7.60$, $P = 0.0086$). Quantitatively, ΔGPP/ER can be predicted based on the fixed effects in the model as $\Delta\text{GPP/ER} = 0.46 - 0.45 \times \text{GPP/ER} - 0.019 \times \text{Temperature}$.

To establish how warming is likely to affect the metabolic balance in streams globally, we assembled a stream metabolism data set of daily GPP, ER, and mean water temperature based on two previous synthesis studies[32,44], and applied the linear model for ΔGPP/ER as a function of both GPP/ER and mean water temperature to the compiled data set. We selected data within the range of daily GPP/ER (0.016–0.978) and daily mean temperature (2.2–26.3 °C) found in our study, resulting in a total of 236 metabolism estimates (see supplementary materials). After quantifying the GPP/ER under a 1 °C increase in temperature for streams in the compiled data set, two patterns of warming–induced changes in stream metabolic balance emerged. First, the GPP/ER of streams converged under a 1 °C temperature increase, shown as a decrease in the inter-site variability of GPP/ER (Fig. 4(a)). Second, the convergence in metabolic balance is asymmetric. The magnitude of decrease in GPP/ER in streams with high temperatures and high daily GPP/ER was larger than the magnitude of increase in GPP/ER in streams with low temperatures and low daily GPP/ER. Such asymmetry suggests that warming will influence the metabolic balance of streams with high temperature and daily GPP/ER more substantially, which translates to such streams

becoming stronger carbon sources (i.e. lower GPP/ER).

Implications for the global carbon cycle

We quantified warming–induced changes in NEP, the difference between GPP and ER, based on the simulated warming experiment. We estimated that a 1 °C increase in temperature will increase GPP from 0.89 to 1.12 (g O_2 m^{-2} day^{-1}), and ER from 3.45 to 4.27 (g O_2 m^{-2} day^{-1}) on average across the streams we studied. Scaling our findings to similarly sized streams globally with an estimated benthic area of 2.75×10^5 (km^2)[7,45], a photosynthetic quotient of 1.2 (molar ratio of O_2 to C), and a respiratory quotient of 0.85 (molar ratio of C to O_2)[46], we predict that streams will become 23.6% more heterotrophic, with NEP shifting from -0.0822 to -0.1016 (Pg C $year^{-1}$) globally (Table 1,Fig. 4(c)), in response to a 1 °C increase in temperature. Although our prediction of shifting toward more net heterotrophy in response to warming is consistent with predictions based on metabolic theory[10], it differs importantly in that it results from the asymmetric convergence of metabolic balance, not a universal shift towards heterotrophy for all streams (Fig. 4(d)).

The predictions for how GPP/ER and NEP will change with warming do not come without caveats. The predicted changes in GPP/ER and NEP are based on temperature sensitivity of metabolism for the current state of stream ecosystems, and changes in streams and adjacent terrestrial ecosystems concurrent with warming may complicate this prediction. For example, warming is expected to change the quantity and quality of allochthonous carbon inputs by stimulating soil organic matter decomposition[47] and altering riparian communities[48]. Thermal adaptation of benthic communities[49] and changes in hydrology or nutrient availability[30,50] may further amplify or damp the predicted convergence of metabolic balance. Despite these caveats, our predictions are based on findings from streams that encompass a broad range of biotic and abiotic conditions, which provide a robust basis for assessing the effects of warming on stream metabolic balance across the globe. Incorporating the warming response of stream metabolic balance identified in this study into comprehensive analyses will improve our ability to quantify the feedback between carbon dynamics in streams and future climate changes.

Methods

Study sites and data collection

We conducted this study in six watersheds representing distinct biomes, including tropical forest (LUQ), tropical savanna (AUS), tallgrass prairie (KNZ), temperate rainforest (AND), boreal forest (CPC), and arctic tundra (ARC). Within each watershed, we selected 6–12 streams across a range of stream sizes to capture the physical gradients within the watershed. A detailed description of the study sites can be found in previous work[51]. In each stream, we recorded DO concentration, water temperature, and barometric pressure using a YSI ProODO handheld optical DO meter (YSI Instruments, Yellow Springs, Ohio, USA), and photosynthetically active radiation using an Odyssey Irradiance logger (DataFlowSystems, Christchurch, New Zealand) at a single location in each stream. The DO meter was calibrated with water saturated air immediately before deployment. The readings from the irradiance logger were converted to photosynthetically active radiation based on comparison with a calibrated sensor. We recorded these data at an interval of 5 minutes (ARC) or 10 minutes (all other sites) for 1–14 days. We collected data during base flow periods (Feburary–March 2013 and March 2014 for LUQ, July–August 2013 for AUS, May–June 2013 and April–June 2014 for KNZ, July–August 2015 for AND, July–August 2013 and 2014 for CPC, July–August 2013 and 2014 for ARC). In total, we collected 709 daily DO trajectories from 69 stream reaches across the six biomes.

Estimating activation energies of GPP and ER

We modeled the dynamics of DO concentration with equations 1–4 and employed a Bayesian approach for parameter estimation[39,52–54]. Specifically, for a given set of parameters, we used the Runge-Kutta 4th order method implemented in the R package `deSolve`[55] with a step size of 2.5 minutes to numerically solve the differential equations describing DO dynamics (equations 1–4) and obtained a trajectory of modeled DO concentration. Numerically solving the differential equations with high accuracy requires the interpolation of discrete measurements of light and temperature. To this end, we used linear interpolation to approximate continuous trajectories of light and temperature from discrete measurements. We assumed that the differences between modeled and measured DO were independent and identically distributed normal random errors. Based on this assumption of error distribution, we computed the likelihood for any given set of parameters. We used uniform priors for all parameters in

the model, setting the lower bound of the uniform priors at 0 and upper bound at values significantly larger than found in previous studies to ensure that the posterior inferences were not overly constrained by the prior distributions. In particular, we set the upper bound of the uniform prior for E_{ap} and E_{ar} at 1000 KJ mol^{-1}, which is significantly higher than found in existing literature[19,21–23,25,27,28]. We used Markov Chain Monte Carlo to sample the posterior distributions of the parameters. Specifically, we implemented the adaptive random walk Metropolis-Hasting algorithm[56] with the function `metrop` in R package `mcmc`[57]. We ran each Markov chain for half a million iterations and used a burn-in period of 300000 iterations to ensure stationarity. We performed visual inspection and Geweke diagnostic[58] of the trace plots with R package `coda`[59] for proper mixing and convergence of the Markov chains. All parameters in the model (i.e. P_{max}, R_{T_0}, α, E_{ap}, E_{ar}, K_{20}) were simultaneously estimated. We used posterior means of the parameters for further statistical analyses.

We made two special considerations when estimating parameters. First, low diel variability in temperature in some streams prevented us from estimating E_{ap} and E_{ar} with confidence. Thus, we only used E_{ap} and E_{ar} estimates with 95% highest posterior density intervals narrower than 500 KJ mol^{-1} for further statistical analyses. This is to ensure that the estimated E_{ap} and E_{ar} are mainly determined by the data, not by the uniform priors. With this selection criteria, we obtained 292 estimated E_{ap} and E_{ar} from 48 reaches based on the 709 daily DO trajectories collected from 69 reaches. The choice of 500 KJ mol^{-1} as the threshold is arbitrary. Such an arbitrary choice influences the number of estimated E_{ap} and E_{ar} for further statistical analyses, but does not affect the findings of this study (Fig. S6). Second, when estimating parameters, we divided the data from the same stream into individual days, and estimated a unique set of parameters for each stream on each day, considering the potential for day to day variation of the parameters for the same stream.

To obtain the posterior distributions of daily GPP and ER, we numerically integrated the instantaneous rates of GPP and ER over a day based on each iteration of parameters in the Markov Chain. We performed the same diagnostics of Markov chains to ensure stationarity, proper mixing, and convergence. We obtained the posterior distributions of GPP/ER by taking the ratio of the trace of daily GPP and ER. We reported the means of posterior distributions as point estimates for daily GPP, ER, and GPP/ER. The estimated E_{ap}, E_{ar}, daily GPP, ER, and basic site information are included in the supplementary materials.

Simulated warming experiment

With parameter estimates in the DO model (equations 1–4) for the 292 days of metabolism, we performed a simulated warming experiment to assess the response of stream metabolic balance to temperature increase. We added 1 °C to each individual measurement of water temperature. This warming scenario represents a 1 °C increase in daily mean temperature without changing the daily temperature variability. Using the estimated parameters in the DO model, the observed light trajectories, and the elevated temperature trajectories, we calculated the daily GPP and ER under this warming scenario following the same procedure outlined above. We performed the same diagnostics of the trace plots of daily GPP and ER in the simulated warming experiment. In total, we successfully calculated 288 daily GPP and ER under the 1 °C warming scenario. The daily GPP and ER under the current temperature and the 1 °C warming scenario were used to calculate the proportional change in GPP/ER (ΔGPP/ER) as:

$$\Delta GPP/ER = \frac{GPP/ER_{warming} - GPP/ER_{current}}{GPP/ER_{current}}, \tag{6}$$

where $GPP/ER_{current}$ and $GPP/ER_{warming}$ are daily GPP/ER currently and under the 1 °C warming scenario respectively. The relationship between ΔGPP/ER, currently daily GPP/ER, and mean daily stream temperature was then applied to the global metabolism data set to calculate GPP/ER under 1 °C warming.

We also used results from the simulated warming experiment to evaluate how warming influences NEP in streams globally. Since we measured metabolism for several days in each stream, we first calculated the average GPP and ER for each stream over time and then the average GPP and ER over all streams with a 1 °C increase in temperature. The broad range of biotic and abiotic conditions encompassed in the streams we studied provided a robust basis to extrapolate globally. Thus, we scaled up the average GPP and ER across the streams in our study to a global scale using an estimated benthic area of 2.75×10^5 km^2 for similarly sized streams globally[7,45]. The estimated global stream area corresponded to 1–5th order streams, and is appropriate for the size range of streams we sampled in this study. Finally, we converted metabolism from units of oxygen to carbon using a photosynthetic quotient of 1.2 (molar ratio of O_2 to C) and a respiratory quotient of 0.85 (molar ratio of C to O_2)[46].

Statistical analyses

We analyzed the pattern of $E_{ap} - E_{ar}$ as a function of current daily GPP/ER and daily mean temperature with a linear mixed effects model. Since we estimated a unique set of activation energies for each stream on each day, estimates of multiple days from the same stream could be correlated. Therefore, we included random effects of each stream nested in biome in the model to account for the repeated measurements. We treated the same streams measured in different years as different streams when specifying the random effects. Specifically, we started with a full model and performed backwards model selection to build the most parsimonious model. The fixed effects of the full model included daily GPP/ER, daily mean water temperature, and their interaction. The random effects of the full model included a random intercept and random slopes of both daily GPP/ER and mean water temperature for stream nested in biome. We first fit the full model using maximum likelihood and selected the structure of random effects based on AIC. We found that eliminating the biome-specific random slopes and intercepts lead to a slight decrease in AIC ($\Delta\text{AIC} = -0.86$), but eliminating the stream-level random intercepts ($\Delta\text{AIC} = 54.4$), random slopes of daily GPP/ER ($\Delta\text{AIC} = 22.7$), or random slope of daily mean water temperature ($\Delta\text{AIC} = 10.8$) all resulted in substantial increases in AIC. Therefore, we ultimately specified the random effects with a random intercept and random slopes of GPP/ER and mean water temperature for each stream in our final model. We then refit the model with restricted maximum likelihood and used F-tests with Kenward-Roger approximation of degrees of freedom[60] to select the fixed effects. We found no significant interaction between daily GPP/ER and mean water temperature ($F_{1,25.71} = 0.24$, $P = 0.63$). Thus, the most parsimonious model included daily GPP/ER and mean water temperature as fixed effects, and a random intercept and slopes of both daily GPP/ER and mean water temperature for each stream. We tested whether the fixed effects slopes of daily GPP/ER and mean water temperature were zero using F-test with Kenward-Roger approximation of degree of freedom to evaluate whether daily GPP/ER or mean water temperature had a significant effect on $E_{ap} - E_{ar}$.

Given that the percentage change in reaction rate is proportional to the activation energy in the Arrhenius equation[40], and that $E_{ap} - E_{ar}$ is the activation energy of GPP/ER (equation 5), it follows that predictors of $E_{ap} - E_{ar}$ should also be predictors of ΔGPP/ER. Therefore, we analyzed the effects of daily GPP/ER and mean water temperature on ΔGPP/ER using the same modeling structure as the most parsimonious model for $E_{ap} - E_{ar}$ without

performing the model selection. We fit all the linear mixed effects models using function `lmer` in R package `lme4`[61]. F-test with Kenward-Roger approximation of degrees of freedom was implemented using R package `pbkrtest`[62]. All statistical analyses were performed in R 3.4.1[63].

Data availability

The compiled metabolism data and estimates of activation energies, GPP, and ER from streams we sampled are available in the supplementary information files.

References

1. Battin, T. J. *et al.* The boundless carbon cycle. *Nature Geoscience* **2**, 598–600 (2009).

2. Butman, D. *et al.* Aquatic carbon cycling in the conterminous United States and implications for terrestrial carbon accounting. *Proceedings of the National Academy of Sciences* **113**, 58–63 (2016).

3. Cole, J. J. *et al.* Plumbing the global carbon cycle: integrating inland waters into the terrestrial carbon budget. *Ecosystems* **10**, 172–185 (2007).

4. Raymond, P. A. *et al.* Global carbon dioxide emissions from inland waters. *Nature* **503**, 355–359 (2013).

5. Ciais, P. *et al.* Carbon and other biogeochemical cycles. In Stocker, T. *et al.* (eds.) *Climate Change 2013: the Physical Science Basis. Contribution of Working Group I to the Fifth Assessment Report of the Intergovernmental Panel on Climate Change*, 465–570 (Cambridge University Press, Cambridge, UK, 2013).

6. Hotchkiss, E. *et al.* Sources of and processes controlling CO_2 emissions change with the size of streams and rivers. *Nature Geoscience* **8**, 696–699 (2015).

7. Battin, T. J. *et al.* Biophysical controls on organic carbon fluxes in fluvial networks. *Nature Geoscience* **1**, 95–100 (2008).

8. Kaushal, S. S. *et al.* Rising stream and river temperatures in the United States. *Frontiers in Ecology and the Environment* **8**, 461–466 (2010).

9. Mohseni, O., Erickson, T. R. & Stefan, H. G. Sensitivity of stream temperatures in the United States to air temperatures projected under a global warming scenario. *Water Resources Research* **35**, 3723–3733 (1999).

10. Allen, A., Gillooly, J. & Brown, J. Linking the global carbon cycle to individual metabolism. *Functional Ecology* **19**, 202–213 (2005).

11. Galmes, J., Kapralov, M., Copolovici, L., Hermida-Carrera, C. & Niinemets, Ü. Temperature responses of the Rubisco maximum carboxylase activity across domains of life: phylogenetic signals, trade-offs, and importance for carbon gain. *Photosynthesis research* **123**, 183–201 (2015).

12. Chen, B. & Laws, E. A. Is there a difference of temperature sensitivity between marine phytoplankton and heterotrophs? *Limnology and Oceanography* **62**, 806–817 (2017).

13. Follstad Shah, J. J. *et al.* Global synthesis of the temperature sensitivity of leaf litter breakdown in streams and rivers. *Global change biology* **23**, 3064–3075 (2017).

14. Duan, S.-W. & Kaushal, S. Warming increases carbon and nutrient fluxes from sediments in streams across land use. *Biogeosciences* **10**, 1193–1207 (2013).

15. Raven, J. A. & Geider, R. J. Temperature and algal growth. *New phytologist* **110**, 441–461 (1988).

16. Anderson-Teixeira, K. J., Vitousek, P. M. & Brown, J. H. Amplified temperature dependence in ecosystems developing on the lava flows of Mauna Loa, Hawai'i. *Proceedings of the National Academy of Sciences* **105**, 228–233 (2008).

17. Sand-Jensen, K., Pedersen, N. L. & Søndergaard, M. Bacterial metabolism in small temperate streams under contemporary and future climates. *Freshwater Biology* **52**, 2340–2353 (2007).

18. López-Urrutia, Á. & Morán, X. A. G. Resource limitation of bacterial production distorts the temperature dependence of oceanic carbon cycling. *Ecology* **88**, 817–822 (2007).

19. Welter, J. R. *et al.* Does N_2 fixation amplify the temperature dependence of ecosystem metabolism? *Ecology* **96**, 603–610 (2015).

20. Boyero, L. *et al.* A global experiment suggests climate warming will not accelerate litter decomposition in streams but might reduce carbon sequestration. *Ecology Letters* **14**, 289–294 (2011).

21. Acuna, V., Wolf, A., Uehlinger, U. & Tockner, K. Temperature dependence of stream benthic respiration in an alpine river network under global warming. *Freshwater Biology* **53**, 2076–2088 (2008).

22. Jankowski, K., Schindler, D. & Lisi, P. Temperature sensitivity of community respiration rates in streams is associated with watershed geomorphic features. *Ecology* **95**, 2707–2714 (2014).

460 23. Yvon-Durocher, G., Jones, J. I., Trimmer, M., Woodward, G. & Montoya, J. M. Warm-
461 ing alters the metabolic balance of ecosystems. *Philosophical Transactions of the Royal*
462 *Society B: Biological Sciences* **365**, 2117–2126 (2010).

463 24. Sinsabaugh, R. L. Large-scale trends for stream benthic respiration. *Journal of the*
464 *North American Benthological Society* **16**, 119–122 (1997).

465 25. Yvon-Durocher, G. *et al.* Reconciling the temperature dependence of respiration across
466 timescales and ecosystem types. *Nature* **487**, 472–476 (2012).

467 26. Huryn, A. D., Benstead, J. P. & Parker, S. M. Seasonal changes in light availability mod-
468 ify the temperature dependence of ecosystem metabolism in an arctic stream. *Ecology*
469 **95**, 2826–2839 (2014).

470 27. Demars, B. O. *et al.* Temperature and the metabolic balance of streams. *Freshwater*
471 *Biology* **56**, 1106–1121 (2011).

472 28. Perkins, D. M. *et al.* Consistent temperature dependence of respiration across ecosystems
473 contrasting in thermal history. *Global Change Biology* **18**, 1300–1311 (2012).

474 29. Demars, B., Manson, J., Olafsson, J., Gislason, G. & Friberg, N. Stream hydraulics and
475 temperature determine the metabolism of geothermal icelandic streams. *Knowledge and*
476 *Management of Aquatic Ecosystems* **402**, 1–17 (2011).

477 30. Cross, W. F., Hood, J. M., Benstead, J. P., Huryn, A. D. & Nelson, D. Interactions be-
478 tween temperature and nutrients across levels of ecological organization. *Global Change*
479 *Biology* **21**, 1025–1040 (2015).

480 31. Williamson, T. J. *et al.* Warming alters coupled carbon and nutrient cycles in experi-
481 mental streams. *Global Change Biology* **22**, 2152–2164 (2016).

482 32. Demars, B. O. *et al.* Impact of warming on CO_2 emissions from streams countered by
483 aquatic photosynthesis. *Nature Geoscience* (2016).

484 33. Holtgrieve, G. W., Schindler, D. E. & Jankowski, K. Comment on Demars et al. 2015,
485 "Stream metabolism and the open diel oxygen method: principles, practice, and per-
486 spectives". *Limnology and Oceanography: Methods* **14**, 110–113 (2016).

34. Mahecha, M. D. *et al.* Global convergence in the temperature sensitivity of respiration at ecosystem level. *Science* **329**, 838–840 (2010).

35. American Public Health Association. *Standard methods for the examination of water and wastewater* (American Public Health Association, American Waterworkds Association and Water Environment Federation, Washington, DC, 1995), 19 edn.

36. Jassby, A. D. & Platt, T. Mathematical formulation of the relationship between photosynthesis and light for phytoplankton. *Limnology and Oceanography* **21**, 540–547 (1976).

37. Parkhill, K. L. & Gulliver, J. S. Modeling the effect of light on whole-stream respiration. *Ecological Modelling* **117**, 333–342 (1999).

38. Bott, T. L. Primary productivity and community respiration. In Hauer, F. R. & Lamberti, G. A. (eds.) *Methods in Stream Ecology*, 533–556 (Academic Press, San Diego, California, 2006).

39. Song, C., Dodds, W. K., Trentman, M. T., Rüegg, J. & Ballantyne, F. Methods of approximation influence aquatic ecosystem metabolism estimates. *Limnology and Oceanography: Methods* **14**, 557–569 (2016).

40. Sierra, C. A. Temperature sensitivity of organic matter decomposition in the Arrhenius equation: some theoretical considerations. *Biogeochemistry* **108**, 1–15 (2012).

41. Descamps-Julien, B. & Gonzalez, A. Stable coexistence in a fluctuating environment: an experimental demonstration. *Ecology* **86**, 2815–2824 (2005).

42. Jiang, L. & Morin, P. J. Temperature fluctuation facilitates coexistence of competing species in experimental microbial communities. *Journal of Animal Ecology* **76**, 660–668 (2007).

43. Chesson, P. Mechanisms of maintenance of species diversity. *Annual review of Ecology and Systematics* **31**, 343–366 (2000).

44. Hoellein, T. J., Bruesewitz, D. A. & Richardson, D. C. Revisiting odum (1956): a synthesis of aquatic ecosystem metabolism. *Limnology and Oceanography* **58**, 2089–2100 (2013).

45. Wollheim, W. M. *et al.* Global N removal by freshwater aquatic systems using a spatially distributed, within–basin approach. *Global Biogeochemical Cycles* **22**, GB2026 (2008).

46. Wetzel, R. G. & Likens, G. E. *Limnological Analysis* (Springer, Berlin, Germany, 2013), 3 edn.

47. Freeman, C., Evans, C., Monteith, D., Reynolds, B. & Fenner, N. Export of organic carbon from peat soils. *Nature* **412**, 785–785 (2001).

48. Kominoski, J. S. *et al.* Forecasting functional implications of global changes in riparian plant communities. *Frontiers in Ecology and the Environment* **11**, 423–432 (2013).

49. Padfield, D., Yvon-Durocher, G., Buckling, A., Jennings, S. & Yvon-Durocher, G. Rapid evolution of metabolic traits explains thermal adaptation in phytoplankton. *Ecology Letters* **19**, 133–142 (2016).

50. Demars, B. O., Thompson, J. & Manson, J. R. Stream metabolism and the open diel oxygen method: Principles, practice, and perspectives. *Limnology and Oceanography: Methods* **13**, 356–374 (2015).

51. Rüegg, J. *et al.* Baseflow physical characteristics differ at multiple spatial scales in stream networks across diverse biomes. *Landscape Ecology* **31**, 119–136 (2016).

52. Holtgrieve, G. W., Schindler, D. E., Branch, T. A. & A'mar, Z. T. Simultaneous quantification of aquatic ecosystem metabolism and reaeration using a bayesian statistical model of oxygen dynamics. *Limnology and Oceanography* **55**, 1047–1063 (2010).

53. Riley, A. J. & Dodds, W. K. Whole-stream metabolism: strategies for measuring and modeling diel trends of dissolved oxygen. *Freshwater Science* **32**, 56–69 (2012).

54. Grace, M. R. *et al.* Fast processing of diel oxygen curves: Estimating stream metabolism with BASE (BAyesian Single-station Estimation). *Limnology and Oceanography: Methods* **13**, 103–114 (2015).

55. Soetaert, K., Petzoldt, T. & Setzer, R. W. Solving differential equations in R: package desolve. *Journal of Statistical Software* **33**, 1–25 (2010).

56. Haario, H., Saksman, E. & Tamminen, J. An adaptive metropolis algorithm. *Bernoulli* 223–242 (2001).

57. Geyer, C. J. & Johnson, L. T. *mcmc: Markov Chain Monte Carlo* (2014). R package version 0.9–3.

58. Geweke, J. Evaluating the accuracy of sampling-based approaches to calculating posterior moments. In Bernado, J., Berger, J., Dawid, A. & Smith, A. (eds.) *Bayesian Statistics 4*, 169–193 (Clarendon Press, Oxford, UK, 1992).

59. Plummer, M., Best, N., Cowles, K. & Vines, K. CODA: convergence diagnosis and output analysis for MCMC. *R news* **6**, 7–11 (2006).

60. Kenward, M. G. & Roger, J. H. Small sample inference for fixed effects from restricted maximum likelihood. *Biometrics* 983–997 (1997).

61. Bates, D., Mächler, M., Bolker, B. & Walker, S. Fitting linear mixed-effects models using lme4. *Journal of Statistical Software* **67**, 1–48 (2015).

62. Halekoh, U. & Højsgaard, S. A kenward-roger approximation and parametric bootstrap methods for tests in linear mixed models – the R package pbkrtest. *Journal of Statistical Software* **59**, 1–30 (2014).

63. R Core Team. *R: a language and environment for statistical computing*. R Foundation for Statistical Computing, Vienna, Austria (2017).

Acknowledgements

We thank Keith Gido for his contribution in obtaining funding and designing the field experiments. Keith Gido, John Drake, Craig Osenberg, and Jeff Minucci provided comments on earlier versions of this paper. Georgia Advanced Computing Resource Center provided the computing facility. This study is supported by National Science Foundation grant EF–1258994 and is part of the Scale, Consumers and Lotic Ecosystem Rates project supported by National Science Foundation grant EF–1065255.

Corresponding author

Correspondence and requests for materials should be addressed to Chao Song by email address: chaosong@uga.edu.

Author contributions

C.S. and F.B. conceived the modeling approach to estimating temperature sensitivity. C.S. performed the metabolism modeling, conducted the data analyses, and wrote the manuscript. W.K.D., J.R., A.A., W.B.B., M.M.D., M.B.F., E.A.G., A.M.H., T.K.H., J.B.J., J.S.K., W.H.M., A.D.R., M.R.W., W.M.W., and F.B. designed the field experiments. W.K.D., A.A., W.B.B., M.B.F., T.K.H., J.B.J., J.S.K., W.H.M., A.D.R., M.R.W., W.M.W., and F.B. obtained funding. J.R., A.A., C.L.B., E.A.G., L.E.K., D.M., S.P.P., C.M.R., K.R.S., and M.T.T. collected the data. S.J. and J.R. managed the database. All authors provided feedback on the manuscript.

Competing financial interests

The authors declare no competing financial interests.

Tables

	GPP	ER	NEP
Current	0.0281 ± 0.0036	0.1103 ± 0.0151	-0.0822 ± 0.0127
1°C warming	0.0351 ± 0.0046	0.1367 ± 0.0200	-0.1016 ± 0.0172

Figure captions

Table 1: Global estimates of stream GPP, ER, and NEP currently and under 1 °C increase in temperature. Data are shown as mean±standard error of mean. Unit is Pg C year^{-1}.

Figure 1: Ecosystem–level activation energies of GPP and ER in streams. Each point represents estimated E_{ap} and E_{ar} in a particular stream reach on one day. Histograms on the axes show the frequency distributions of E_{ap} and E_{ar}. Dashed lines are the medians of the frequency distributions.

Figure 2: Relationship between $E_{ap} - E_{ar}$, (a) current GPP/ER and (b) mean daily temperature. Dashed lines are predictions based on fixed effects in the linear mixed effects model ($E_{ap} - E_{ar} = 236.92 - 221.20 \times \text{GPP/ER} - 11.86 \times \text{Temperature}$). In each panel, the prediction line is evaluated at the mean of the other covariate.

Figure 3: Proportional change in GPP/ER under 1 °C warming as a function of (a) current daily GPP/ER and (b) mean water temperature. Dashed lines are predictions based on fixed effects in the linear mixed effects model ($\Delta\text{GPP/ER} = 0.46 - 0.45 \times \text{GPP/ER} - 0.019 \times \text{Temperature}$). In each panel, the prediction line is evaluated at the mean of the other covariate.

Figure 4: Predicted changes in GPP/ER and NEP under 1 °C warming. Frequency distribution of (a) GPP/ER and (c) NEP currently and with a 1 °C increase in temperature. Changes in (b) GPP/ER and (d) NEP with a 1 °C increase in temperature. The dashed line in (c) is the isocline defined by the fixed effects from the linear mixed effects model ($0.46 - 0.45 \times \text{GPP/ER} - 0.019 \times \text{Temperature} = 0$), where GPP/ER is insensitive to temperature changes.

Figure 1: Activation energies of GPP and ER in streams. Each point represents estimated E_{ap} and E_{ar} in a particular stream reach on one day. Histograms on the axes show the frequency distributions of E_{ap} and E_{ar}. Dashed lines are the median E_{ap} and E_{ar}.

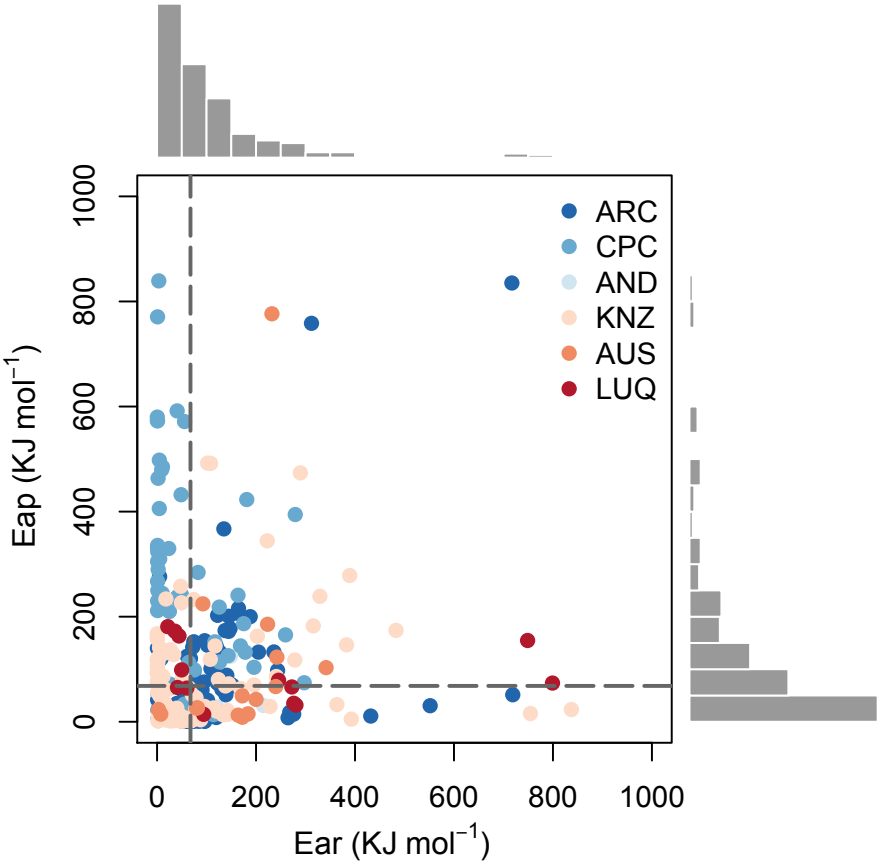

Figure 2: Relationship between $E_{ap} - E_{ar}$, (a) current GPP/ER and (b) mean daily temperature. Dashed lines are predictions based on fixed effects in the linear mixed effects model ($E_{ap} - E_{ar} = 236.92 - 221.20 \times \text{GPP/ER} - 11.86 \times \text{Temperature}$). The prediction line is evaluated at the mean of the other covariate.

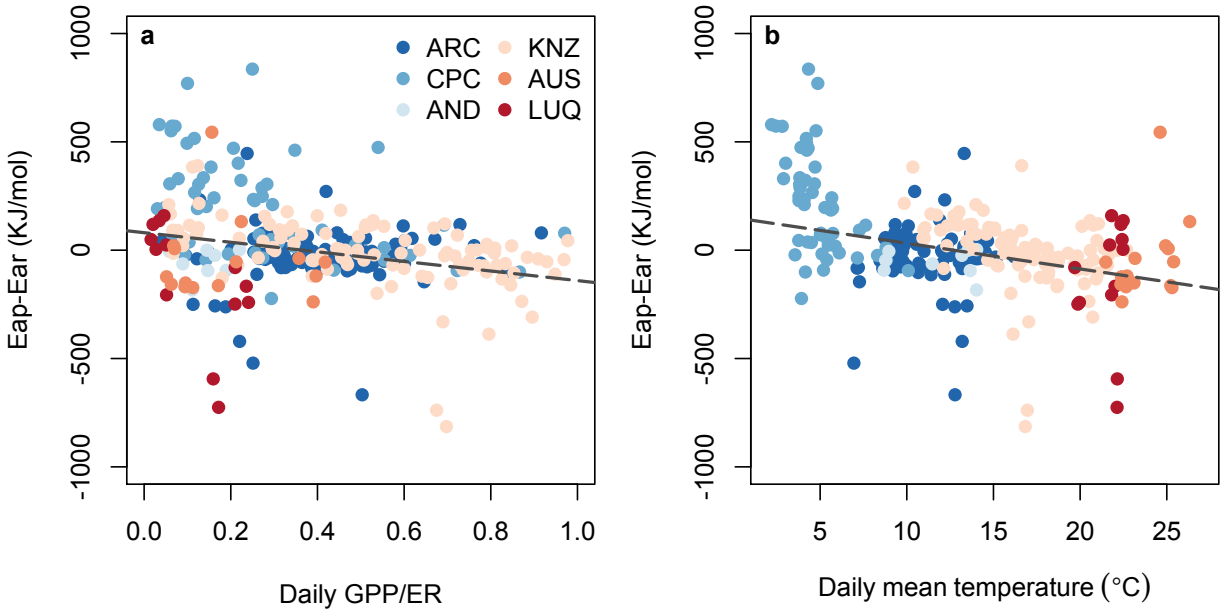

Figure 3: Proportional change in GPP/ER under 1 °C warming as a function of (a) current daily GPP/ER and (b) mean water temperature. Dashed lines are predictions based on fixed effects in the linear mixed effects model (ΔGPP/ER = 0.46 − 0.45 × GPP/ER − 0.019 × Temperature). The prediction line is evaluated at the mean of the other covariate.

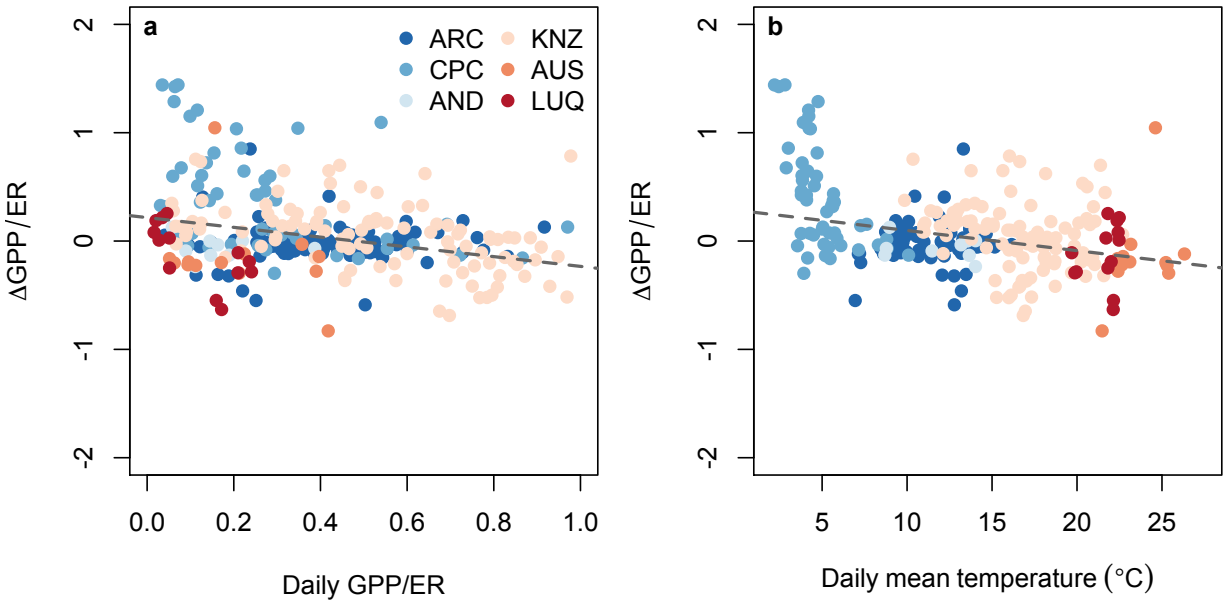

Figure 4: Predicted changes in GPP/ER and NEP under 1 °C warming. Frequency distribution of (a) GPP/ER and (c) NEP currently and with a 1 °C increase in temperature. Changes in (b) GPP/ER and (d) NEP with a 1 °C increase in temperature. Dashed line in (c) is the isocline defined by the fixed effects from the linear mixed effects model ($0.46 - 0.45 \times \text{GPP/ER} - 0.019 \times \text{Temperature} = 0$), where GPP/ER is insensitive to temperature changes.